



Published in final edited form as:

J Neuropathol Exp Neurol. 2008 July ; 67(7): 677–686. doi:10.1097/NEN.0b013e31817e5c5e.

Oxidative Injury in the Cerebral Cortex and Subplate Neurons in Periventricular Leukomalacia

Rebecca D. Folkerth, MD^{1,2,3}, Felicia L. Trachtenberg, PhD⁴, and Robin L. Haynes, PhD^{1,3}

¹ Department of Pathology, Children's Hospital, Boston, Massachusetts

² Department of Pathology, Brigham and Women's Hospital, Boston, Massachusetts

³ Harvard Medical School, Boston, Massachusetts

⁴ New England Research Institutes, Watertown, Massachusetts

Abstract

We previously identified immunocytochemical evidence of nitrative and oxidative injury in premyelinating oligodendrocytes in periventricular leukomalacia (PVL). Here, we tested the hypothesis that free radical injury occurs in the overlying cerebral cortex and subplate neurons in PVL. We immunostained for nitrotyrosine (NT), malondialdehyde (MDA), and hydroxynonenal (HNE) adducts and scored neuron staining density in PVL (n = 11) and non-PVL (n = 15) cases (postconceptional ages from 34 to 109 weeks). Analysis of covariance controlled for age. Mean MDA scores in PVL cases were increased over controls (p = 0.005). HNE scores increased with age only in PVL cases (diagnosis versus age interaction, p = 0.024). NT scores were not significantly increased. In 11 PVL and 23 control cases between 20 and 183 postconceptional weeks, cells morphologically consistent with subplate and Cajal-Retzius neurons showed qualitatively increased free radical modification in PVL over control cases with statistically significant odds ratios for HNE and NT in both subplate neurons and Cajal-Retzius cells. GFAP and CD68 scores for reactive astrocytes and microglia, respectively, were not significantly increased, suggesting a minimal inflammatory response. Thus, oxidative/nitrative damage to cortical and "pioneer" neurons, although mild overall, may contribute to cortical volume loss and cognitive/behavioral impairment in survivors of prematurity.

Keywords

Cerebral palsy; Dendritogenesis; Free radical injury; Prematurity; Synaptogenesis

INTRODUCTION

Periventricular leukomalacia (PVL), the major neuropathological substrate of the motor deficits of cerebral palsy, is characterized by focal periventricular necrosis and diffuse gliosis in the surrounding immature white matter. Preterm infants with and without PVL also develop significant cognitive and behavioral abnormalities (1). In premature infants weighing less than 1500 g at birth, for example, 25% to 50% will develop cognitive impairments ranging in severity from subtle learning disabilities to mental retardation (1). Term-born infants with congenital heart or respiratory disease also are at risk for PVL and its complications (2). Recently, we noted the previously under-emphasized occurrence of cerebral gray matter gliosis

and neuronal loss in autopsy cases of PVL in the modern era of neonatal intensive care (3). Neuroimaging studies likewise indicate reduced cerebral cortical gray matter volume in premature infants studied at term equivalent, with or without PVL, compared to term control infants (4,5). Furthermore, several studies report reduced cortical volumes that correlate with gestational age at birth and neurodevelopmental disability (4–10).

Although the pathogenesis of PVL is multifactorial, a major cause appears to be cerebral ischemia/reperfusion in the immature white matter that preferentially targets vulnerable premyelinating oligodendroglial cells (11–13). These cells are characterized by expression of O4 and O1, but not myelin basic protein and are susceptible to free radical injury in PVL (14,15). Here, we hypothesized that subtle oxidative and nitrative injury to the developing cerebral cortical gray matter, subplate-like neurons, and/or layer I neurons (including Cajal-Retzius-like cells) is also present in the brains of infants dying with PVL, compared to controls of similar ages who died without PVL. We evaluated the degree of oxidative and nitrative injury in neurons in the cerebral cortex (layers I, III, and V) and subplate in postmortem brain specimens in cases with and without PVL using immunocytochemical methods on the same dataset (i.e. same tissue sections) in which we had found significant levels of such injury in the white matter (15). We applied antibodies against MDA and 4-hydroxy-2-nonenal (HNE) (markers of lipid peroxidation), nitrotyrosine (NT) (a marker of protein nitration), as well as CD68 (a macrophage/microglia marker), and glial fibrillary acidic protein (GFAP) (a marker for reactive astrocytes), as previously published (15). The latter two antibodies are used commonly in diagnostic neuropathology practice and were included as indicators of cellular response to neuronal injury. Since microglia are sources of nitric oxide (NO) and peroxynitrite, and contribute to developing oligodendrocyte injury and death (16,17), we also sought to determine whether microglial activation was associated with the markers of nitrative and/or oxidative stress.

MATERIALS AND METHODS

Clinicopathologic Database Information

Cases were collected from the autopsy services of the Departments of Pathology, Children's Hospital and Brigham and Women's Hospital, Boston, with permission according to hospital protocols. All cases were autopsied between 1993 and 2001 and were classified by the systematic examination of standardized microscopic sections (maximum of 19 sections/case), stained with hematoxylin-and-eosin/Luxol-fast-blue (H&E/LFB), from each brain and spinal cord (the latter available on 8 cases). We defined PVL based upon the combination of "focal" and "diffuse" components, as determined by gross and microscopic examination (18). The focal component consists of periventricular necrosis, in which all tissue elements are destroyed, analogous to the "core" of an infarct. The diffuse component is comprised of reactive gliosis and microglial activation in the deep white matter surrounding the necrotic foci. The areas of predilection for PVL are the frontal, parietal, and occipital white matter regions. Acute PVL is identified histopathologically by coagulative necrosis, characterized by nuclear pyknosis (shrinking) of all cell types and axonal swellings (spheroids), and corresponds to injury within the preceding 8 to 24 hours (18). Subacute or organizing PVL develops between 3 and 5 days following the insult and is identified by infiltration of activated microglia, macrophages, and hypertrophic astrocytes at the onset of tissue loss and cavitation (18). Chronic PVL is recognized as cystic cavitation, glial scar formation, and/or mineralization associated with diffuse astro- and microgliosis, within weeks to months following the insult (18). Control cases were defined by the absence of PVL upon gross and microscopic neuropathologic examination. Among the PVL cases, we selected blocks for study from areas of the brain affected only by periventricular leukomalacia, because some cases had gray matter injury elsewhere in the brain (Table 1B). Since our hypothesis addressed the question of subtle, sublethal injury to the cortex,

rather than overt, direct injury that would result in frank infarct or laminar necrosis, we excluded from analysis any blocks with diffuse cortical injury.

Eleven PVL cases (34–95 postconceptional weeks) and 23 control cases (i.e. lacking the focal necrosis of PVL) (20–183 postconceptional weeks) had brain tissue fixed in formalin and embedded in paraffin; these tissues were used for single-labeling immunocytochemistry. The PVL cases and controls are the same as those used in our previous analysis of oxidative and nitrative injury in the cerebral white matter (15), except for 3 of the PVL cases (Cases 2–4), which were excluded from the current analysis for technical reasons (e.g. technically inadequate staining of entire tissue section, i.e. the cortex; insufficient cortex in the block, etc.). We additionally stained 1 case (40 gestational and 4 postnatal weeks, or 44 postconceptional weeks of age) with a recent organizing segmental cortical infarct for comparative purposes and to be certain that we could detect evidence of free radical damage in cerebral cortex, that is, a “positive control.”

In view of the nature of an autopsy series from a tertiary care pediatric hospital, the extent of associated pathology among the PVL cases and controls is broad (15). Nevertheless, brain blocks were chosen to be representative of the presence or absence of neuropathology in PVL and control cases, respectively. Five PVL and 5 control cases had also been subjected to the intensive survey of gray matter injury reported previously (3). “Cortex overlying PVL” was defined as the segment of cortex nearest the foci of periventricular necrosis associated with diffuse white matter gliosis. When the section orientation allowed, the segment of cortex counted was located radially along a perpendicular line from the ventricular to the pial surface. Postmortem interval for the entire cohort ranged from 1.5 to 132 hours, with a mean of 18.3 and a median of 14 hours. There was no obvious effect of postmortem interval upon the degree of immunostaining. Statistical analyses were also performed to determine the effect of postmortem interval on the scored staining results.

Immunocytochemistry in Formalin-Fixed, Paraffin-Embedded Tissue

Standard methods on deparaffinized tissue sections (4 μm) were applied, as previously described (15). Antibodies specific for the following markers were used at the indicated dilutions: 4-hydroxy-2-nonenal-protein adducts (HNE) (1:100; from the laboratory of Dr. Luke I. Szewda, or purchased from Calbiochem, San Diego, CA); malondialdehyde protein adducts (MDA) (1:100; Abcam, Cambridge, UK); nitrotyrosine protein adducts (NT) (1:100; Upstate, Lake Placid, NY); glial fibrillary acidic protein (GFAP) (1:9000, Sternberger Monoclonals Incorporated, Lutherville, MD), and CD68 (1:50, Cell Marque, Austin, TX). These were characterized for their specificity as previously reported (15). Optimal dilutions were determined using Alzheimer and amyotrophic lateral sclerosis brain and spinal cord tissue, in which free radical injury is known to occur, as positive controls. “Positive” control staining consisted of the glial immunoreactivity in the white matter in the same blocks, as previously reported (15). In addition, a case with a segmental cortical infarct was stained as a “positive” neuronal control. Tonsil was used as the positive control for CD68 immunostaining; negative controls were the omission of the primary antibodies. To check for nonspecific staining, we preabsorbed the NT antibody at a concentration of 1:100 with 50 μg of 3-nitro-L-tyrosine (Sigma-Aldrich) in 150 ml PBS containing 4% normal goat serum, for 5 hours at room temperature. After preabsorption, the antibody-NT solution was substituted for primary antibody on tissue prepared for immunocytochemistry, and incubated overnight at 4°C; DAB detection was then performed as described.

Grading Method and Statistical Analysis

Grading of the immunostained tissue sections was performed by counting positive cells per high-power field (hpf) at x400 magnification (0.173 mm^2 on an Olympus BH-2 microscope),

as previously in the white matter in the same immunostained tissue sections (15). The hpf's were selected on the basis of the greatest density of immunostaining after visual survey of all fields at low magnification. Immunostaining was cytoplasmic for all the antibodies analyzed. Positively stained neurons were counted if they were located within layers II–VI of the cerebral cortex. The grading system was as follows: 0, no cell staining; 1/2, 1 immunopositive cell/hpf; 1, 2 to 10 cells/hpf; 2, 11 to 20 immunopositive cells/hpf; and 3, >20 cells/hpf, according to our published protocol (15,19–21). For assessment of the immunostaining of the subplate and Cajal-Retzius neurons a binary scheme was used as follows: 0, no staining; 1, staining of the specific cell type present. Subplate neurons and Cajal-Retzius cells were separately scored according to this grading system because the densities of these cell types are relatively low and they are not amenable to the cell counting procedure used in the cerebral cortex in which neurons are more densely packed. Cajal-Retzius cells were identified by their characteristic large, polygonal appearances, and their localization in layer I and along the pial surface. Care was taken not to overcount Cajal-Retzius cells at the tissue edge, which might be artifactually overstained (“edge effect”). Subplate neurons occupied “layer VII”, just deep to layer VI, and had multipolar, bipolar, or unipolar morphologies as previously described (22). Separate counting of the different cell types was not done. In view of the lack of specific markers for these 2 cell types in human archival material, we relied on histomorphology, recognizing that the terms “subplate-like” and Cajal-Retzius-like” may be more appropriate. To simplify discussion, however, we use the shorter designations in this report. Two observers scored each case without knowledge of clinical variables, including age. Since the presence of focal necrosis and diffuse gliosis are the defining features of PVL, however, blinding to this diagnosis was not possible.

Analysis of covariance was performed to test for significant differences in marker scores between PVL and control cases, controlling for postconceptional age. Cases (n = 11) and controls (n = 15) over similar developmental intervals (34–109 postconceptional weeks) were used for the cortical neuron density values and cases over the entire age range (n = 11 PVL and 23 controls, 20–183 postconceptional weeks) were used for the binary subplate and Cajal-Retzius values. If there was a significant interaction between diagnosis and age it was included in the model. Correlations between markers in the cortex and white matter were calculated. The latter values were previously published as a separate report (15). Additionally, regressions of postmortem interval, as well as postnatal age, on markers were performed. Finally, the Spearman correlation of subplate and Cajal-Retzius immunostaining to cortical immunostaining was computed. In all analyses, $p < 0.05$ was considered significant; values between 0.05 and 0.10 were considered to indicate a trend. Because of the exploratory nature of this work, we report p values between 0.05 and 0.10.

RESULTS

Clinical and Neuropathologic Findings

Findings are summarized in Tables 1A and 1B. The PVL cases ranged in postconceptional age from 34 to 95 weeks (median = 40 weeks) and the controls ranged from 20 to 183 postconceptional weeks (median = 40 weeks). Nine of the 11 PVL cases (81.8%) were born prematurely (<37 weeks); 3 of these 9 infants survived beyond the neonatal period (>44 postconceptional weeks). In the control group, 9/23 (39.1%) were born prematurely but none survived beyond the perinatal period. The prematurely born PVL cases had Potter syndrome/renal dysplasia (n = 3), skeletal dysplasia (n = 2), complications of prematurity (n = 2), and congenital heart disease and pulmonary hypertension (n = 1 each) (15). The clinical courses of the full-term PVL infants were complicated by an inborn error of the urea cycle in 1 case, and congenital heart malformation requiring surgery and extracorporeal membrane oxygenation in another (15). In 6 PVL cases, focal cystic cavities measuring up to 3 mm were

visible macroscopically in the periventricular white matter. Microscopically, 4 cases had acute coagulative necrosis characterized by fragmentation of all tissue elements and pyknotic or absent nuclei, indicative of an acute insult of 24 to 48 hours duration (18); 7 cases had necrotic foci with subacute changes (i.e. with infiltration of macrophages and beginning cavitation) (18); and 7 cases had chronic changes (i.e. cyst, glial scarring, or mineralization) indicating the site of prior focal necrosis (18). Five cases had focal lesions of more than 1 histopathologic age. Six PVL cases had expanded ventricles and/or decreased white matter volume, and 3 had hypomyelination; these cases all had either organizing or chronic PVL lesions (15). Affected lobes from which blocks were used for this study included parietal (n = 4), parieto-occipital (n = 1), occipital (n = 1), and frontal (n = 2); 3 blocks were from cerebral cortex, not otherwise specified. With respect to gray matter injury among the PVL cases, one had focal neuronal loss associated with focal cortical hemorrhage, and one had a focal cortical infarct; for both cases, the lesions were in a different section than the one graded semiquantitatively in the study. In the blocks used for immunohistochemistry, the overlying cortex was free of hypoxic-ischemic injury by light microscopy.

In the cases without PVL, 4 were extremely premature and had respiratory insufficiency and/or necrotizing enterocolitis; one was born at 35 weeks and died of germinal matrix hemorrhage. The other 4 premature controls had a congenital cardiac anomaly (n = 2, one as a component of the VACTERL association), one had parvovirus-associated anemia and hydrops, and one was an unexplained stillbirth at 34 weeks. Of the controls born at term, 2 had congenital heart disease, 2 had congenital renal dysplasia, 3 had a chromosomal abnormality (trisomy 21, 12–14 translocation, Noonan syndrome; n = 1 each), and 1 each had spinal muscular atrophy, pulmonary hypoplasia, pulmonary hypertension, primary biliary atresia (status post liver transplant), viral gastroenteritis and dehydration, sudden unexpected death in childhood, and bronchopneumonia. As in the PVL cases, cerebral cortical blocks were free of infarcts, inflammation, or significant hemorrhage. Control cortex and white matter blocks were chosen on the basis of availability of periventricular white matter and well-oriented overlying cortex; they were comparable in size to those obtained from PVL cases. The locations included parietal lobe (n = 4), occipital lobe (n = 2), frontal lobe (n = 7), and cerebral cortex, not otherwise specified (n = 10).

In the case with the cortical infarct used as a “positive” control, the gestational age was 40 weeks, postnatal age 4 weeks, and postconceptional age 44 weeks. The infant had an unattended delivery with asphyxia and was found to have a congenital diaphragmatic hernia, requiring extracorporeal membrane oxygenation. Although the child also had PVL, the block chosen for comparative staining contained an infarct of several days duration; this case was not scored.

Markers of Free Radical Injury in PVL and Non-PVL Cortex

Overall, there was mild oxidative and nitrative injury as determined by immunostaining of layer V, and to a lesser extent layer III, pyramidal neurons (Fig. 1A–C). This injury was detectable as individual immunopositive neurons within these layers in the cerebral cortical ribbon present on the section and by variable immunostaining of the background neuropil. By semiquantitative scoring, PVL cases showed age-adjusted mean scores for MDA immunostaining in cortical neurons of 0.65 (range 0–2, median 1), whereas controls showed age-adjusted means for of 0.06 (range 0–1, median 0) ($p = 0.005$) (Table 1; Fig. 2). In the age range studied, PVL HNE scores were significantly higher than control HNE scores ($p = 0.024$) (Table 1; Fig. 3), with an increase in HNE score with age only for PVL cases. The effect of postconceptional age was most striking within the first 60 postconceptional weeks but only one PVL case was examined beyond that time point. Therefore, conclusions past ~60 postconceptional weeks are tentative. Nitrotyrosine immunostaining was present in cerebral cortical neurons in only two PVL cases (mean score 0.22, range 0–1, median 0) (Fig. 1C),

while none of the controls were labeled, a marginal difference ($p = 0.091$) (Table 1, Figure 2). Staining in the cortex overlying PVL was qualitatively less than that seen in a representative section of a cortical infarct (Fig. 1E). Negative controls (omission of primary antibody and excess protein preabsorption) demonstrated no staining (data not shown).

We next addressed the question of whether free radical injury in the cortex overlying PVL correlates with the degree of free radical injury in the white matter (Fig. 1F) that we previously documented (15), but no significant relationship was identified between the white matter and cortex scores for any of the markers used (data not shown). To determine whether infants that survived longer had greater degrees of cortical injury, the effect of postnatal age on the study population was explored, but we found no influence of postnatal age (either as a continuous variable or in analysis restricted to cases with postnatal age greater than 5 days) on marker scores in the cortex (data not shown). Likewise, no effect of gestational age (i.e. degree of maturity at birth) or of postmortem intervals on marker scores were identified (data not shown).

The subplate was stained by at least one free radical adduct marker in 10/11 PVL cases, with 5 cases immunostained for all 3 markers (Fig. 4A; Table 2A). Cajal-Retzius neurons were also immunopositive for at least one of these markers in 9/11 PVL cases and in 3 cases for all 3 markers (Fig. 4B; Table 2B). For both cell populations, approximately 2- to 3-fold increases in number of positive cells were detected for each marker in PVL versus control cases (Table 2A, B). Of note, in control cases, subplate and Cajal-Retzius cells were immunopositive for HNE and MDA, even if there was no staining of cortical layers II-VI (Table 2A, B). Subplate and Cajal-Retzius neurons showed qualitatively increased evidence of free radical modification in PVL cases over controls, with statistically significant odds ratios of 20.9 (CI 2.2, 199) for HNE and 9.1 (CI 1.3, 63.1) for NT in subplate neurons, and 12.6 (CI 1.2, 135) for HNE and 7.3 (CI 1.2, 45.1) for NT in Cajal-Retzius cells (Table 3).

Markers of Inflammatory Reaction in the Cerebral Cortex Overlying PVL

Fibrillary gliosis assessed by GFAP staining was mild in the cerebral cortex overlying PVL (Figs. 1G, 2). The age-adjusted mean scores of GFAP-positive astrocytes in the cortex in the PVL cases was 0.97 (range 0–3, median 0.5), compared to a mean score of 0.39 (range 0–1, median 0) in the controls ($p = 0.100$) (Table 1). Anti-CD68 staining showed variable densities of immunopositive reactive microglia in the PVL cortex, with an age-adjusted mean score of 0.73 (range 0–1, median 1), compared to 0.33 for controls (range 0–2, median 0) ($p = 0.060$) (Figs. 1H, 2). There was no significant correlation between any of the oxidative and nitrative marker scores and the scores for the inflammatory cell markers (data not shown).

DISCUSSION

The major finding of this study is the presence of oxidative and nitrative injury in the cerebral cortex overlying PVL, and in subplate neurons and Cajal-Retzius cells. This finding, albeit subtle, supports the occurrence of mild gray matter as well as white matter injury in PVL. The concept of gray matter injury in PVL is not entirely new but it is gaining in importance as prematurely born infants survive longer and reach school age, and cognitive and behavioral deficits emerge that are not readily explained by cerebral white matter damage alone (1,23). Thus, interest has arisen concerning the extent, associations, and causes of such gray matter injury. Quantitative magnetic resonance (MR) imaging data suggest a significant reduction in cerebral cortical volume in premature infants studied at term equivalent, compared to term infants, a finding that is especially pronounced in infants with PVL (4,5). In our own investigation of the neuropathology of prematurity in the modern era of intensive care, we have detected widespread and variable gliosis and neuronal loss in centers involved in cognitive processing (i.e. cerebral cortex, thalamus, and cerebellar relay nuclei) in infants with PVL (3). While the gliosis and neuronal loss in that cohort varied from mild to severe, they suggest

a heretofore under-emphasized vulnerability of the immature gray matter, in addition to the well-recognized vulnerability of the developing white matter (12,24). This has prompted us to coin the term “perinatal panencephalopathy.”

In the current study, we hypothesized that the cerebral cortex overlying PVL undergoes cellular modification by free radicals, given the findings by us (25) and others (26,27) for a role for free radicals in the pathogenesis of the white matter injury. We therefore assessed, in a semiquantitative fashion, the density of cells showing immunopositivity for markers of oxidative and nitrative injury (hydroxynonenal, malondialdehyde, and nitrotyrosine), as well as standard neurohistologic markers of cell reactions (i.e. GFAP for astrocytes and CD68 for microglia/macrophages) in a dataset that we had already analyzed similarly for evidence of white matter injury (25). We found that MDA-positive cell density in neurons in layers II–VI was mildly but significantly elevated compared to controls adjusted for postconceptional age. We also found a significant increase in HNE-immunopositive cells with increasing postconceptional age in PVL, in contrast to controls, in whom the density remained constant with increasing age, (i.e. age versus diagnosis interaction). In contrast, neither of the standard neuropathological markers of gliosis (GFAP) or microglial activation (CD68) consistently identified differences between PVLs and controls, although there were trends toward significance. This result supports the contention that the cerebral cortex is *relatively* spared in reference to the white matter in PVL (25). The degree of free radical injury to other gray matter sites (e.g. thalamus) is the focus of ongoing work in the laboratory.

The reasons for the disparity between the markers of oxidative stress and the inflammatory markers of injury are uncertain, but could include a time window necessary for the free radicals to stimulate microglial and astrocytic response, or some inherent limitation in the capability of the cortex to respond that contrasts with the marked GFAP and CD68 response in the injured white matter in PVL at this age (25). It is also noteworthy that we were not able to identify a correlation between postnatal age (survival time) and cerebral cortical marker scores indicating that infants who survive longer did not necessarily have more injury. In addition, if the injury to the cortical neurons is sublethal, astrocytic and microglial reactions may be more modest than in the areas of frank neuronal necrosis.

Might the microglial response to injury in the cerebral cortex of the premature infant be developmentally regulated? Across normal development, the density of activated microglia is transiently higher in the cerebral white matter of the fetus or premature infant (<37 postconceptional weeks) relative to the term infant, as well as to the overlying cortex in either age group (19). This developmental pattern suggests a basis, at least in part, for the increased free radical injury in white matter relative to cortex (i.e. the normal transient increase in microglia may “prime” the white matter for injury in the occurrence of hypoxia-ischemia) and give rise to proliferation of activated CD68-positive microglia seen in the diffuse component of PVL (25). Microglia generate peroxynitrite via inducible nitric oxide synthase and superoxide via NADPH oxidase, leading to oligodendrocyte free radical injury (15,26) and death (17). Although less dense in the cerebral cortex than in the white matter, it is possible that when they are exposed to hypoxia-ischemia, cytokines, and excitotoxicity, cortical microglia could also generate sufficient free radicals to cause adduct formation in scattered neurons overlying PVL.

Vulnerability to Free Radical Injury

The localization of free radical marker immunostaining to layer V, and to a lesser degree, layer III neurons in this study was striking. It is possible that the visibility of staining could have been enhanced in these neurons because of their more abundant cytoplasm, versus the smaller, granular or compact cells of the other layers. This localization may, however, reflect a differential susceptibility of these neurons compared to those in layers II, IV, and VI within

the cerebral cortex. Between 25 and 37 postconceptional weeks, in deep layers of the cortical plate, glutamate receptor subunit 1 expression is high while glutamate receptor subunit 2 (gluR2) expression is low, a receptor configuration that confers increased vulnerability to calcium-permeable excitotoxicity to neurons in that location (28). Nearer term and in the postnatal period, (i.e. 38–46 postconceptional weeks), cortical pyramidal and non-pyramidal neurons in all layers express low levels of gluR2, relative to subunit 1 (28). We speculate that the developmental association for HNE (age \times diagnosis interaction; [i.e. the older the infant with PVL, the greater the cerebral cortical labeling with HNE]) may reflect a component of development-related vulnerability to excitotoxicity and the subsequent generation of oxygen free radicals and membrane adduct formation. The findings could also indicate a greater capability to produce free radicals with age, for example, increased metabolic capacity. It is noteworthy that the HNE staining in controls was always 0, regardless of age, indicating the need potentially for a pathological inciting event, such as hypoxia-ischemia, excitotoxicity, and/or cytokine toxicity.

The qualitative patterns of subplate and Cajal-Retzius cell staining may reflect a particular susceptibility of these early-born “pioneer” neurons to free radical injury. Overall, the markers HNE and NT were increased 2- to 3-fold in PVL over controls in subplate neurons, and HNE and MDA were similarly increased in Cajal-Retzius neurons. Of note, during the developmental period studied, subplate neurons and Cajal-Retzius cells are relatively deficient in gluR2 subunit, rendering them susceptible to calcium-permeable excitotoxicity (28) (D.M. Talos, personal communication). In addition, these cells express nitric oxide synthase (29,30) and this could explain, at least in the subplate, the basis for NT modification in our cohort.

The potential consequences of injury to the subplate and Cajal-Retzius (layer I) neurons in PVL is of great interest with respect to the cognitive and behavioral deficits in survivors of prematurity and the volumetric gray matter losses identified on quantitative neuroimaging. Subplate and Cajal-Retzius cells are required for normal organization and function of the developing cortex (31,32), and may retain a modulatory role in the adult rat cortex (33,34). As discussed below, free radicals could induce loss or dysfunction of these neurons at critical periods in thalamocortical or corticothalamic axonal outgrowth and synaptogenesis. In the human telencephalon, the subplate population is thought to have its peak density during the PVL window of vulnerability (24–32 postconceptional weeks) (35), functioning as a “waiting zone” for ingrowing afferents to the cortical plate (36). These afferents penetrate the cortical plate at a time of intense dendritic differentiation of deep cortical neurons (28–30 gestational weeks) (36). The fate of subplate neurons in PVL has been open to conjecture (37), and potential effects of free radicals on the subplate, as in the cortical plate itself, include cell death as well as sublethal injury interfering with afferent ingrowth and dendritic arborization. Subplate neurons are known to be selectively vulnerable to hypoxia-ischemia in rodents (38) and they can be ablated in the developing cat using kainate excitotoxicity (32), but injury to subplate neurons in the human by free radicals has to our knowledge not been demonstrated.

Differences Between Cerebral Cortical and White Matter Injury Due to Free Radicals The absolute increase in marker scores in the white matter compared to the cortex in PVL raises the question of whether “more” free radical injury might be occurring in the white matter. The possible explanation for this difference could include the relative hypovascularization of the white matter (as an end-arterial zone) compared to the cerebral cortex (39). In addition, oligodendrocytes are a rich source of iron and are postulated to play a part in the Fenton reaction that creates increased hydroxyl radicals in the setting of ischemia and reperfusion (11,40). The immaturity of antioxidant systems in the white matter also likely contributes to a disparity in the vulnerability of the white matter to oxidative and nitrative injury (41–43). This contrasts to the relatively early expression of antioxidant enzymes in the developing cortex (44) (Folkerth, unpublished observations). Also, white matter astrocytes and subplate neurons, as

well as white matter microglia, may be sources of nitric oxide and superoxide and hence nitrative and oxidative injury (29).

Comparisons with Animal Models

The pattern of oxidative modification of cerebral neurons in our cohort resembles that described in a fetal sheep model of hypoxic-ischemic brain injury (45). In that model, HNE immunostaining was found in the cerebral cortex, along with other gray and white matter sites in the experimental group that had undergone umbilical cord occlusion; this staining was completely absent in controls. Specifically, HNE adducts were observed in layers II–V of the parietal cortex; Cajal-Retzius and subplate neurons were not described. In a rat cerebrocortical slice system, NT was detected in neurons by immunohistochemistry after hypoxia as well as NMDA exposure and was attenuated by the NMDA antagonist MK-801 (46). That study illustrates the convergence of hypoxic-ischemic and excitotoxic factors in the pathogenesis of free radical injury in the brain.

Potential Mechanisms of Cortical Injury and Volume Loss

How might subtle free radical injury to the developing cortex contribute to cortical volume loss (i.e. thinning on quantitative MR)? The 2 main postulated mechanisms requiring investigation include 1) neuronal cell loss (in cortex, subplate, or both), via apoptotic and/or necrotic cell death; and 2) sublethal injury to cortical and/or subplate neurons, affecting the subcellular synaptodendritic compartment, i.e. loss of neuropil. We believe that the finding of variable immunostaining of the background neuropil indicates free radical exposure, adduct formation, and potential sublethal injury in the cortex, which may not necessarily lead to gliosis or overt neuronal loss. Of note, in animal models of cerebrovascular disorders, loss of presynaptic markers SNAP-25 and synaptophysin (47), and changes in nerve terminals and dendritic spines (48) have been described. Such changes can be caused directly by the action of oxygen free radicals on the neuronal cytoskeleton, as illustrated *in vitro* by the disruption of neuronal microtubules and microfilaments, and modification of vimentin intermediate filaments and cellular tubulin, leading to disruption of neurite outgrowth (49,50). Future studies directly in postmortem human tissue, many ongoing in our laboratory at this time, will be necessary to determine the relative contributions of cell death and sublethal neuronal injury to gray matter volume loss.

Conclusion

In summary, subtle but significant modification of cerebral cortical neurons by free radicals occurs in the setting of periventricular white matter injury, and lends support to the notion of shared mechanisms of gray and white matter injury in “perinatal panencephalopathy.” While many issues remain to be elucidated, these findings suggest a basis, at least in part, for the loss of cerebral cortical volume in survivors of prematurity and their cognitive difficulties upon reaching school age. They also indicate the need for preventive strategies targeted at sources of free radical injury in the gray matter, as well as white matter, in the newborn.

Acknowledgments

Supporting grants: NINDS PO1-NS38475 and NICHD P30-HD18655 (Children’s Hospital Boston Mental Retardation and Developmental Disabilities Research Center)

Yaman Z. Eksioğlu, MD, PhD, Children’s Hospital Department of Neurology, Boston MA 02115, assisted in the scoring of immunostaining. Richard A. Belliveau, BA, provided expertise with the illustrations. For two control cases, human tissue was obtained from the NICHD Brain and Tissue Bank for Developmental Disorders under contracts NO1-HD-4-3368 and NO1-HD-4-3383. The support and encouragement of Dr. Joseph J. Volpe is gratefully acknowledged.

References

1. Volpe JJ. Cerebral white matter injury of the premature infant-more common than you think. *Pediatrics* 2003;112:176–80. [PubMed: 12837883]
2. Kinney HC, Panigrahy A, Newburger JW, Jonas RA, Sleeper LA. Hypoxic-ischemic brain injury in infants with congenital heart disease dying after cardiac surgery. *Acta Neuropathol (Berl)* 2005;110:563–78. [PubMed: 16244891]
3. Pierson CR, Folkerth RD, Billiards SS, Trachtenberg FL, Drinkwater ME, Volpe JJ, Kinney HC. Gray matter injury associated with periventricular leukomalacia in the premature infant. *Acta Neuropathol (Berl)* 2007;114:619–31. [PubMed: 17912538]
4. Inder TE, Huppi PS, Warfield S, Kikinis R, Zientara P, Barnes PD, et al. Periventricular white matter injury in the premature infant is associated with a reduction in cerebral cortical gray matter volume at term. *Ann Neurol* 1999;46:755–60. [PubMed: 10553993]
5. Inder TE, Warfield SK, Wang H, Huppi PS, Volpe JJ. Abnormal cerebral structure is present at term in premature infants. *Pediatrics* 2005;115:286–94. [PubMed: 15687434]
6. Nosarti C, Al-Asady MHS, Franfou S, Stewart AL, Rifkin L, Murray RM. Adolescents who were born very preterm have decreased brain volume. *Brain* 2002;125:1616–23. [PubMed: 12077010]
7. Peterson BS, Anderson AW, Ehrenkranz R, Staib LH, Tageldin M, Colson E, et al. Regional brain volumes and their later neurodevelopmental correlates in term and preterm infants. *Pediatrics* 2003;111:939–48. [PubMed: 12728069]
8. Peterson BS, Vohr B, Kane MJ, Whalen DH, Schneider KC, Katz KH, et al. A functional magnetic resonance imaging study of language processing and its cognitive correlates in prematurely born children. *Pediatrics* 2002;110:1153–62. [PubMed: 12456913]
9. Peterson BS, Vohr B, Staib LH, Cannistraci CJ, Dolberg A, Schneider KC, et al. Regional brain volume abnormalities and long-term cognitive outcome in preterm infants. *JAMA* 2000;284:1939–47. [PubMed: 11035890]
10. Isaacs EB, Lucas A, Chong WK, Wood SJ, Johnson CL, Marshall C, et al. Hippocampal volume and everyday memory in children of very low birth weight. *Pediatr Res* 2000;47:713–20. [PubMed: 10832727]
11. Volpe JJ. Perinatal brain injury: From pathogenesis to neuroprotection. *MRDD Res Rev* 2001;7:56–64.
12. Volpe JJ. Neurobiology of periventricular leukomalacia in the premature infant. *Pediatr Res* 2001;50:553–62. [PubMed: 11641446]
13. Kinney, HC.; Armstrong, DL. Perinatal Neuropathology. In: Graham, DI.; Lantos, PE., editors. *Greenfield's Neuropathology*. 7. London: Arnold; 2002. p. 557-59.
14. Back SA, Luo NL, Borenstein NS, Levine JM, Volpe JJ, Kinney HC. Late oligodendrocyte progenitors coincide with the developmental window of vulnerability for human perinatal white matter injury. *J Neurosci* 2001;21:1302–12. [PubMed: 11160401]
15. Haynes RL, Folkerth RD, Keefe RJ, Sung I, Swzeda LI, Rosenberg PA, Volpe JJ, Kinney HC. Nitrosative and oxidative injury to premyelinating oligodendrocytes in periventricular leukomalacia. *J Neuropathol Exp Neurol* 2003;62:441–50. [PubMed: 12769184]
16. Xie Z, Wei M, Morgan TE, Fabrizio P, Han D, Finch CE, et al. Peroxynitrite mediates neurotoxicity of amyloid beta-peptide 1–42- and lipopolysaccharide-activated microglia. *J Neurosci* 2002;22:3484–92. [PubMed: 11978825]
17. Li J, Baud O, Vartanian T, Volpe JJ, Rosenberg PA. Peroxynitrite generated by inducible nitric oxide synthase and NADPH oxidase mediates microglial toxicity to oligodendrocytes. *Proc Natl Acad Sci U S A* 2005;102:9936–41. [PubMed: 15998743]
18. Kinney, HC.; Haynes, RL.; Folkerth, RD. White matter disorders in the perinatal period. In: Golden, JA.; Harding, B., editors. *Pathology and Genetics: Acquired and Inherited Diseases of the Developing Nervous System*. Vol. 20. Basel: ISN Neuropathology Press; 2004. p. 29-40.
19. Billiards SS, Haynes RL, Folkerth RD, Trachtenberg FL, Liu LG, Volpe JJ, et al. Development of microglia in the cerebral white matter of the human fetus and infant. *J Comp Neurol* 2006;497:199–208. [PubMed: 16705680]

20. Haynes RL, Folkerth RD, Szweda LI, Volpe JJ, Kinney HC. Lipid peroxidation during human cerebral myelination. *J Neuropathol Exp Neurol* 2006;65:894–904. [PubMed: 16957583]
21. Folkerth RD, Keefe RJ, Haynes RL, Trachtenberg FL, Volpe JJ, Kinney HC. Interferon-gamma expression in periventricular leukomalacia in the human brain. *Brain Pathol* 2004;14:265–74. [PubMed: 15446581]
22. deAzevedo LC, Hedin-Pereira C, Lent R. Callosal neurons in the cingulate cortical plate and subplate of human fetuses. *J Comp Neurol* 1997;386:60–70. [PubMed: 9303525]
23. Volpe JJ. Brain Injury in the Premature Infant-Magnitude of the Problem (Commentary). *J Watch Neurol*. 2000
24. Folkerth RD. Periventricular leukomalacia: Overview and recent findings. *Pediatr Dev Pathol* 2006;9:3–13. [PubMed: 16808630]
25. Haynes RL, Rosenberg PA, Folkerth RD, Volpe JJ, Kinney HC. Expression of inducible nitric oxide synthetase in reactive astrocytes in human periventricular leukomalacia. *Soc for Neurosci Abstr*. 2003
26. Back SA, Luo NL, Mallinson RA, O'Malley JP, Wallen LD, Frei B, et al. Selective vulnerability of preterm white matter to oxidative damage defined by F2-isoprostanes. *Ann Neurol* 2005;58:108–20. [PubMed: 15984031]
27. Inder TE, Mocatta T, Darlow B, Spencer C, Volpe JJ. Elevated free radical products in the cerebrospinal fluid of VLBW infants with cerebral white matter injury. *Pediatr Res* 2002;52:213–18. [PubMed: 12149498]
28. Talos DM, Follett PL, Folkerth RD, Fishman RE, Trachtenberg FL, Volpe JJ, et al. Developmental regulation of alpha-amino-3-hydroxy-5-methyl-4-isoxazole-propionic acid receptor subunit expression in forebrain and relationship to regional susceptibility to hypoxic/ischemic injury. II. Human cerebral white matter and cortex. *J Comp Neurol* 2006;497:61–77. [PubMed: 16680761]
29. Haynes RL, Baud O, Li J, Kinney HC, Volpe JJ, Folkerth DR. Oxidative and nitrative injury in periventricular leukomalacia: A review. *Brain Pathol* 2005;15:225–33. [PubMed: 16196389]
30. Sestan N, Kostovic I. Histochemical localization of nitric oxide synthase in the CNS. *Trends Neurosci* 1994;17:105–6. [PubMed: 7515524]
31. Ghosh A, Antonini A, McConnell SK, Shatz CJ. Requirement for subplate neurons in the formation of thalamocortical connections. *Nature* 1990;347:179–81. [PubMed: 2395469]
32. Ghosh A, Shatz CJ. A role for subplate neurons in the patterning of connections from thalamus to neocortex. *Development* 1993;117:1031–47. [PubMed: 8325233]
33. Hanganu IL, Kilb W, Luhmann HJ. Spontaneous synaptic activity of subplate neurons in neonatal rat somatosensory cortex. *Cereb Cortex* 2001;11:400–10. [PubMed: 11313292]
34. Hanganu IL, Kilb W, Luhmann HJ. Functional synaptic projections onto subplate neurons in neonatal rat somatosensory cortex. *J Neurosci* 2002;22:7165–76. [PubMed: 12177212]
35. Kostovic I, Rakic P. Developmental history of the transient subplate zone in the visual and somatosensory cortex of the macaque monkey and human brain. *J Comp Neurol* 1990;297:441–70. [PubMed: 2398142]
36. Kostovic I, Judas M. Correlation between the sequential growth of afferents and transient patterns of cortical lamination in preterm infants. *Anat Rec* 2002;267:1–6. [PubMed: 11984786]
37. Volpe JJ. Subplate neurons--missing link in brain injury of the premature infant? *Pediatrics* 1996;97:112–13. [PubMed: 8545202]
38. McQuillen PS, Sheldon RA, Shatz CJ, Ferriero DM. Selective vulnerability of subplate neurons after early neonatal hypoxia-ischemia. *J Neurosci* 2003;23:3308–15. [PubMed: 12716938]
39. Rorke LB. Anatomical features of the developing brain implicated in pathogenesis of hypoxic-ischemic injury. *Brain Pathol* 1992;2:211–21. [PubMed: 1343836]
40. Connor JR, Phillips TM, Lakshman MR, Barron KD, Fine RE, Csiza CK. Regional variation in the levels of transferrin in the CNS of normal and myelin-deficient rats. *J Neurochem* 1987;49:1523–29. [PubMed: 3312497]
41. Baud O, Greene AE, Li J, Wang H, Volpe JJ, Rosenberg PA. Glutathione peroxidase-catalase cooperativity is required for resistance to hydrogen peroxide by mature rat oligodendrocytes. *J Neurosci* 2004;24:1531–40. [PubMed: 14973232]

42. Baud O, Haynes RF, Wang H, Folkerth RD, Li J, Volpe JJ, et al. Developmental up-regulation of MnSOD in rat oligodendrocytes confers protection against oxidative injury. *Eur J Neurosci* 2004;20:29–40. [PubMed: 15245476]
43. Folkerth RD, Haynes RL, Wang H, Li J, Volpe JJ, Rosenberg PA, et al. Developmental regulation of manganese superoxide dismutase in rat oligodendrocytes confers protection against glutathione depletion induced toxicity. *Soc Neurosci Abstr* 2004:141.14.
44. Takikawa M, Kato S, Esumi H, Kurashima Y, Hirano A, Asayama K, Nakashima K, Ohama E. Temporospacial relationship between the expressions of superoxide dismutase and nitric oxide synthase in the developing human brain: Immunohistochemical and immunoblotting analyses. *Acta Neuropathol* 2001;102:572–80. [PubMed: 11761717]
45. Castillo-Melendez M, Chow JA, Walker DW. Lipid peroxidation, caspase-3 immunoreactivity, and pyknosis in late-gestation fetal sheep brain after umbilical cord occlusion. *Pediatr Res* 2004;55:864–71. [PubMed: 14764919]
46. Ochiai-Kanai R, Hasegawa K, Takeuchi Y, Yoshioka H, Sawada T. Immunohistochemical nitrotyrosine distribution in neonatal rat cerebrocortical slices during and after hypoxia. *Brain Res* 1999;847:59–70. [PubMed: 10564736]
47. Ishimaru H, Casamenti F, Ueda K, Maruyama Y, Pepeu G. Changes in presynaptic proteins, SNAP-25 and synaptophysin, in the hippocampal CA1 area in ischemic gerbils. *Brain Res* 2001;903:94–101. [PubMed: 11382392]
48. Zhang S, Boyd J, Delaney K, Murphy TH. Rapid reversible changes in dendritic spine structure in vivo gated by the degree of ischemia. *J Neurosci* 2005;25:5333–38. [PubMed: 15930381]
49. Neely MD, Sidell KR, Graham DG, Montine TJ. The lipid peroxidation product 4-hydroxynonenal inhibits neurite outgrowth, disrupts neuronal microtubules, and modifies cellular tubulin. *J Neurochem* 1999;72:2323–33. [PubMed: 10349841]
50. Allani PK, Sum T, Bhansali SG, Mukherjee SK, Sonee M. A comparative study of the effect of oxidative stress on the cytoskeleton in human cortical neurons. *Toxicol Appl Pharmacol* 2004;196:29–36. [PubMed: 15050405]

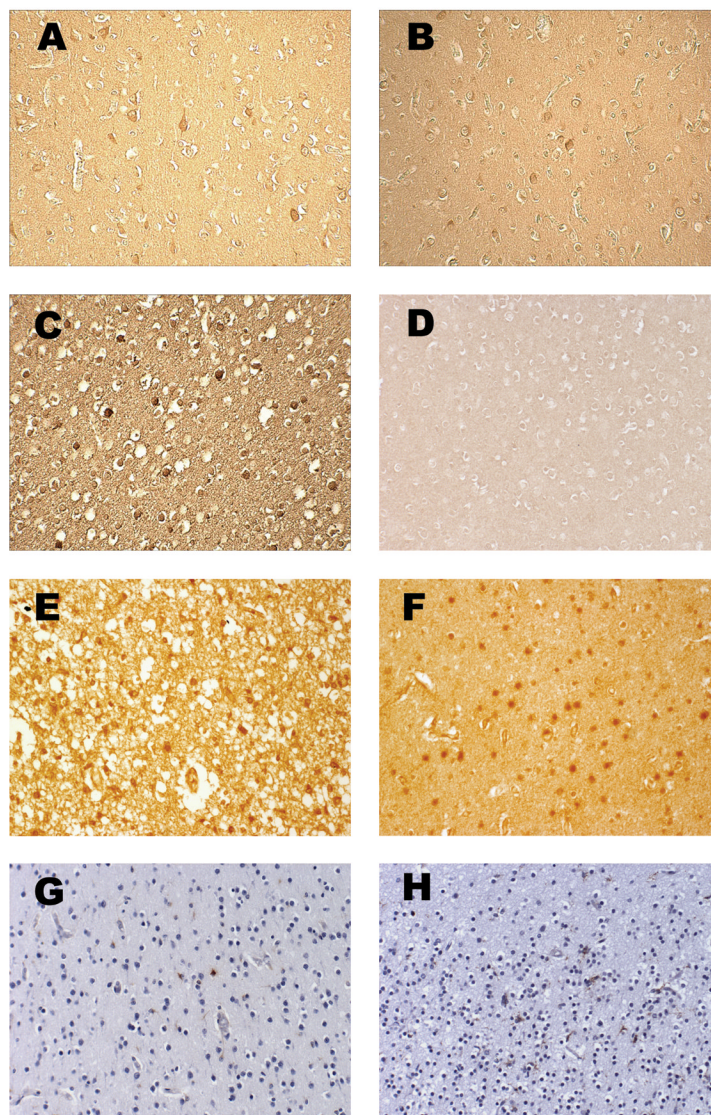


Figure 1. Immunostaining of cerebral cortex with markers of free radical injury and cellular response. (A) Malondialdehyde (MDA) adduct in cytoplasm of scattered cerebral cortical neurons, PVL case aged 95 postconceptional weeks. (B) HNE adduct in neuronal cytoplasm, PVL case aged 95 postconceptional weeks. (C) Nitrotyrosine (NT) in neuronal nucleus and cytoplasm, PVL case aged 40 postconceptional weeks. (D) Hydroxynonenal (HNE) immunostain showing no immunoreactivity in cortical neurons of a non-PVL case aged 54 postconceptional weeks. (E) HNE adduct in a segmental cortical infarct in a “positive control” case aged 44 postconceptional weeks. (F) HNE adduct in the white matter of a PVL case aged 51 weeks. (G) GFAP in astrocytes, PVL case aged 51 postconceptional weeks. (H) CD68 for macrophages, PVL case aged 35 postconceptional weeks. Original magnification: x200 for each. Note the variable immunostaining of the background neuropil, interpreted as free radical adducts involving plasma membranes of cell processes; as expected, this is strongest in the cortical infarct (E), but also notable in (A–C).

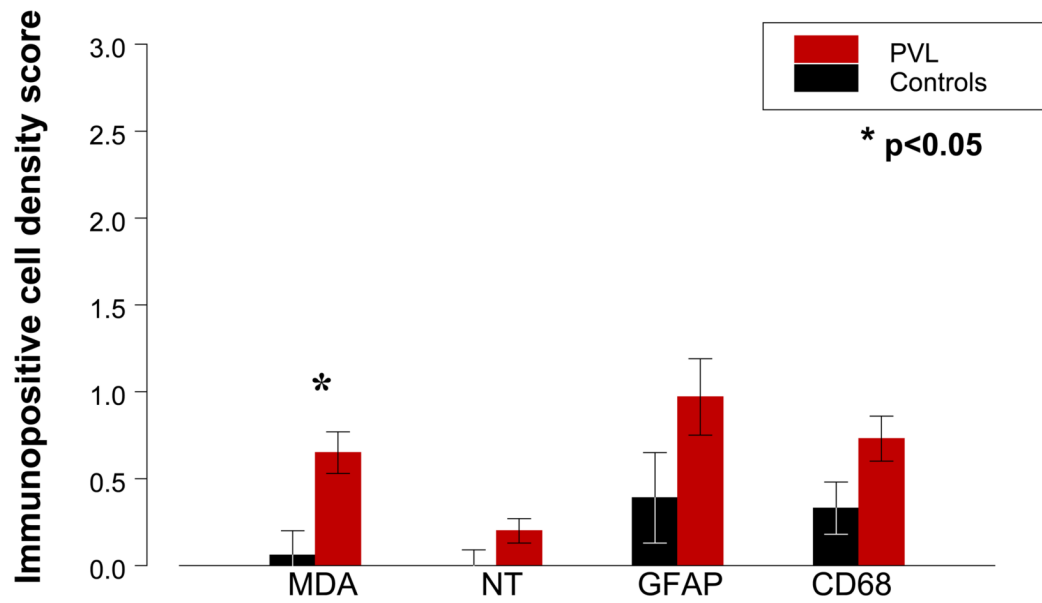


Figure 2. Mean age-adjusted marker scores (see text for score criteria) in cerebral cortex of PVL cases (red bars) and controls (black bars). Note the overall low scores for all markers (each less than 1.0) and that statistical significance is achieved only for MDA, although NT, CD68, and GFAP scores showed a trend toward significance (Table 1).

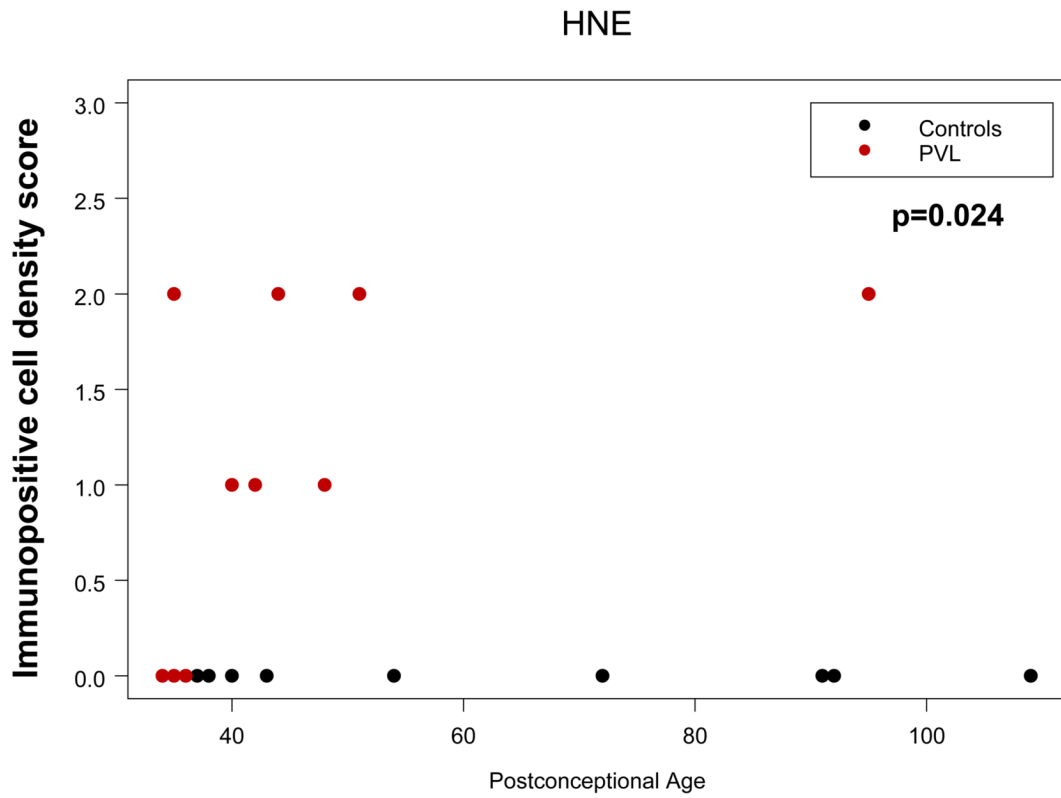


Figure 3.

Relationship between age and HNE marker scores in PVL (XXX dots) versus controls (XXX dots) across 34 to 109 postconceptional weeks. With increasing age, HNE adduct formation increases significantly in the cerebral cortex in PVL but not in controls (see text for discussion).

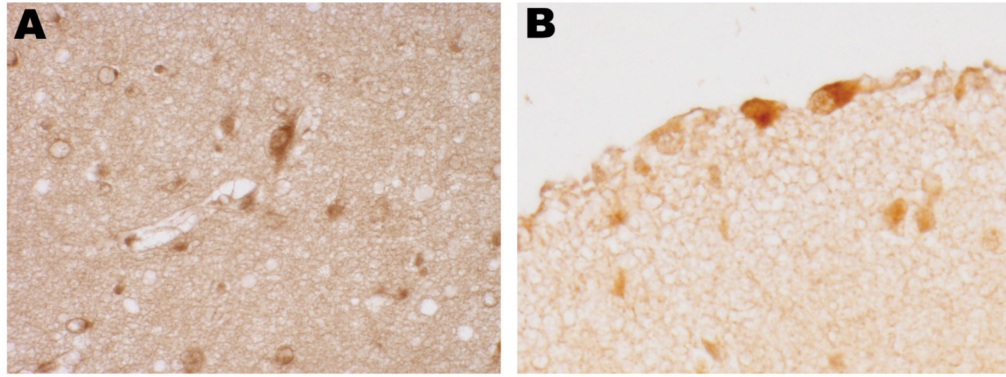


Figure 4. Immunostaining of subplate neurons for HNE (**A**, 40 postconceptional weeks PVL case) and Cajal-Retzius cells for MDA (**B**, 40 postconceptional weeks PVL case). Original magnification: x400 for each.

Table 1

TABLE 1A. Summary of Cerebral White Matter Pathology in PVL cases

Case*	GA	PNA	PCA	Focal Acute Necrosis	Focal Organizing Necrosis	Focal Scar w/Mineral	Diffuse Gliosis	↓WM and/or ↑Vents	Hypo-myelin
1 [^] 0054	35 ^{**}	0	35	+	+	+	+	+	-
5 [^] 9841	34 ^{**}	0	34	-	+	+	+	-	-
6 [^] 9636	28 ^{**}	7	35	+	+	+	+	+	-
7 [^] 9829	36 ^{**}	0	36	-	-	+	+	+	-
8 0006	39	1	40	+	-	-	+	-	-
9 9615	35 ^{**}	5	40	-	+	-	+	-	-
10 9520	36 ^{**}	6	42	-	+	+	+	-	+
11 0053	40	4	44	+	-	-	+	-	-
12 0109	28 ^{**}	20	48	-	-	+	+	+	+
13 [^] 9817	36 ^{**}	15	51	-	+	+	+	+	+
14 9627	31 ^{**}	64	95	-	+	-	+	+	-

TABLE 1B. Continued Summary of the Neuropathology of PVL Cases

Case*	Bst	CB	BG	Thal	Hipp	CCH	WMH	SAH	GMH	Diagnosis
1 [^]	-	-	A, B	-	A	-	-	-	-	Potter syndrome; abnormal temporal lobe gyration; malrotation of hippocampi; duplication of dentate gyrus
5 [^]	-	-	G	G	-	-	-	+	-	Osteogenesis imperfecta
6 [^]	A	-	E, H	E, H	-	-	+	-	-	Necrotizing enterocolitis; bowel perforation; coagulopathy; sepsis
7 [^]	A	I	-	-	-	-	-	-	+	CMV infection in utero; ABO incompatibility; dwarfism/skeletal dysplasia; fetal heart failure
8	-	-	A	-	-	B	-	-	-	Urea cycle defect (ornithine transcarbamylase deficiency); hyperammonemia
9	NA	J	A	A	A	K	+	-	-	Breech birth; oligohydramnios; renal sclerosis

TABLE 1B. Continued Summary of the Neuropathology of PVL Cases

Case*	Bst	CB	BG	Thal	Hipp	CCH	WMH	SAH	GMH	Diagnosis
10	A	L	A	A	-	A	-	-	-	Intrauterine growth retardation; breech birth; oligohydramnios; dysplastic kidneys; malformed basal ganglia and hippocampus
11	A	A	NA	A, M	A	-	-	-	-	Congenital cardiac malformation; ECMO treatment
12	-	-	A	-	-	-	-	-	-	Pulmonary hypertension; pneumonia; ECMO treatment
13 [^]	-	-	-	N	-	-	-	-	-	Breech birth; oligohydramnios; pneumothorax; respiratory failure
14	-	-	-	-	A	-	-	+	+	Congenital cardiac malformation; ECMO treatment

* Case numbers are the same as those used in the prior analysis of white matter (15). Cases 2, 3, and 4 from that study were not included here;

[^] Case was included in a previous gray matter survey (3); GA = gestational age in weeks; PNA = postnatal age in weeks; PCA = postconceptional age in weeks; mineral = mineralization; WM = white matter, Vents = ventricles.

** Prematurity is defined as a gestational age less than 37 weeks; +, present; -, absent.

* Case numbers are the same as those used in the prior analysis of white matter (15) (see Materials and Methods);

[^] Case was included in prior gray matter survey (3); +, pathology present; -, pathology absent; A = reactive gliosis; B = neuronal loss; C = ischemic necrosis; D = hemorrhagic infarct; E = apoptosis; F = focal microhemorrhage; G = mineralization; H = perivascular hemorrhage; I = microglial nodules; J = vermiform nodules; K = organizing infarct; L = Purkinje cell loss; M = microinfarct; N = necrotic focus in hypothalamus; ECMO = extracorporeal membrane oxygenation; NA = not available; Bst, brainstem; BG, basal ganglia; Thal, thalamus; Hipp, hippocampus; CCH, cerebral cortex hemorrhage; WMH, white matter hemorrhage; GMH, germinal matrix hemorrhage.

Table 2
Age-Adjusted Means of Marker Scores in Cerebral Cortical Neurons in PVL and Control Cases

	Age-adjusted mean (SE)			p-value	
	PVL	Controls	PVL v. Controls	PCA	Interaction DX × PCA
MDA	0.65 (0.14)	0.06 (0.12)	0.005	NS	NS
HNE	1.23 (0.15)	0.00 (0.13)	NS	NS	0.024
NT	0.20 (0.09)	0.00 (0.07)	0.091	NS	NS
GFAP	0.97 (0.26)	0.39 (0.22)	0.100	0.099	NS
CD68	0.73 (0.15)	0.33 (0.13)	0.060	0.082	NS

SE = standard error of the mean; PCA = postconceptional age; DX = diagnosis (PVL vs. control); NS = not significant and $p > 0.100$; p values ≥ 0.05 and < 0.100 are included to indicate possible trends for future study; bold type = p value < 0.050 ; - = not applicable. Range of marker scores is 0 (no staining) to 3 (> 20 positive cells/high-power field) (see text for details). Ages of analyzed cases are 34 to 109 postconceptional weeks (see text for details).

Table 3

Table 3A. Subplate Neuron Immunostaining

Marker	Control	PVL
HNE	7/22 (32%)	10/11 (91%)
MDA	11/22 (50%)	9/11 (82%)
NT	2/21 (10%)	5/10 (50%)

Table 3B. Cajal-Retzius Cell Immunostaining

Marker	Control	PVL
HNE	8/19 (42%)	9/10 (90%)
MDA	8/21 (38%)	9/11 (82%)
NT	0/21 (0%)	3/9 (33%)

Numbers in each cell indicate the fraction of cases with positive immunostaining for the marker over the total number of cases with available staining (percentage).

Table 4

Logistic Regression Odds Ratios of Markers in PVLs Versus Controls

	Marker	Odds Ratio [95% confidence interval]	p value
Subplate neurons	HNE	20.92 [2.20, 198.62]	0.008
	MDA	4.66 [0.80, 27.19]	0.087
	NT	9.15 [1.33, 63.11]	0.025
Cajal-Retzius cells	HNE	12.57 [1.17, 135.2]	0.037
	MDA	7.27 [1.17, 45.11]	0.033
	NT	Infinite*	NS

* = all controls have a score of 0; 3 of 9 PVL cases have a score of 1; NS = not significant and > 0.100; p values ≥ 0.05 and < 0.100 are included to indicate possible trends for future study; bold type = p value < 0.050. Ages of analyzed cases are 20 to 183 postconceptional weeks (see text for details).